

Infrared hot-electron NbN superconducting photodetectors for imaging applications

K S Il'in^{†‡}, A A Verevkin[‡], G N Gol'tsman^{†‡} and Roman Sobolewski^{†§}

[†] Department of Electrical and Computer Engineering and Laboratory for Laser Energetics, University of Rochester, Rochester, NY 14627-0231, USA

[‡] Department of Physics, Moscow State Pedagogical University, Moscow 119435, Russia

E-mail: roman@ece.rochester.edu (Roman Sobolewski)

Received 22 June 1999

Abstract. We report an effective quantum efficiency of 340, responsivity $>200 \text{ A W}^{-1}$ ($>10^4 \text{ V W}^{-1}$) and response time of $27 \pm 5 \text{ ps}$ at temperatures close to the superconducting transition for NbN superconducting hot-electron photodetectors (HEPs) in the near-infrared and optical ranges. Our studies were performed on a few nm thick NbN films deposited on sapphire substrates and patterned into μm -size multibrIDGE detector structures, incorporated into a coplanar transmission line. The time-resolved photoresponse was studied by means of subpicosecond electro-optic sampling with 100 fs wide laser pulses. The quantum efficiency and responsivity studies of our photodetectors were conducted using an amplitude-modulated infrared beam, fibre-optically coupled to the device. The observed picosecond response time and the very high efficiency and sensitivity of the NbN HEPs make them an excellent choice for infrared imaging photodetectors and input optical-to-electrical transducers for superconducting digital circuits.

1. Introduction

The quantum efficiency N , responsivity $R_{I,V}$ and the response time constant τ are the main performance parameters used for characterizing optical receivers. For modern semiconducting photodetectors, in the visible wavelengths, all these parameters can independently (i.e. for different devices) reach the following values: $N \leq 100\%$ [1], or up to 30 for effective N for avalanche photodiodes [2], $R_I \sim 1 \text{ A W}^{-1}$ [1] ($R_I \sim 50 \text{ A W}^{-1}$ for avalanche photodiodes [2]) and $\tau < 0.9 \text{ ps}$ [3]. As the radiation wavelength increases, however, it becomes progressively more difficult to implement these ultimate characteristics, especially N and $R_{I,V}$, for semiconducting technology since the photon energy, even for narrow-gap semiconductors, becomes smaller than the gap itself. For that reason, there are practically no semiconducting photodetectors for a significant, and technologically important, far-infrared part of the radiation spectrum.

In this work, we report our studies on the optical response of NbN superconducting hot-electron photodetectors (HEPs). We have measured both the electron energy relaxation time and the response sensitivity of high-quality, 3.5 nm thick NbN films at optical (0.4 μm) and near-infrared (0.79 μm) wavelengths. The effective quantum efficiency

§ Also at the Institute of Physics, Polish Academy of Sciences, PL-02668 Warsaw, Poland.

$N \approx 340$, responsivity $R_I > 200 \text{ A W}^{-1}$, the device response time constant $\tau \approx 30 \text{ ps}$ and electron-phonon scattering time $\tau_{e-ph} = 10 \pm 2 \text{ ps}$ were obtained using the results of our measurements.

2. Experimental details

NbN films with a 3.5 nm thickness were deposited on sapphire substrates by reactive dc magnetron sputtering in an Ar + N₂ gas mixture [4]. The best values of both the critical current density J_c and the transition temperature T_c were achieved at a discharge current of 300 mA, partial N₂ pressure of $1.1 \times 10^{-4} \text{ mbar}$ and substrate temperature of 850 °C. The films were patterned into 4 mm long coplanar waveguide (CPW) structures with a 30 μm wide central line, separated by 6 μm -wide gaps from the ground planes. The tested HEPs consisted of several parallel, μm -wide strips, located in the middle of the CPW, between the central line and the grounds. Vanadium strips terminated both ends of the CPW to ensure 50 Ω output impedance of our device. Typically, after processing, the device exhibited the midpoint of the superconducting transition (definition of T_c) in the 10.3 K–11.7 K range, with $<1 \text{ K}$ transition width, and $J_c = (1.6\text{--}2) \times 10^6 \text{ A cm}^{-2}$ at 4.2 K. The sheet resistance in the normal state was $R_s \approx 200 \Omega \text{ cm}^{-1}$.

The NbN devices were mounted on a copper cold finger inside an exchange-gas, liquid-helium dewar, with

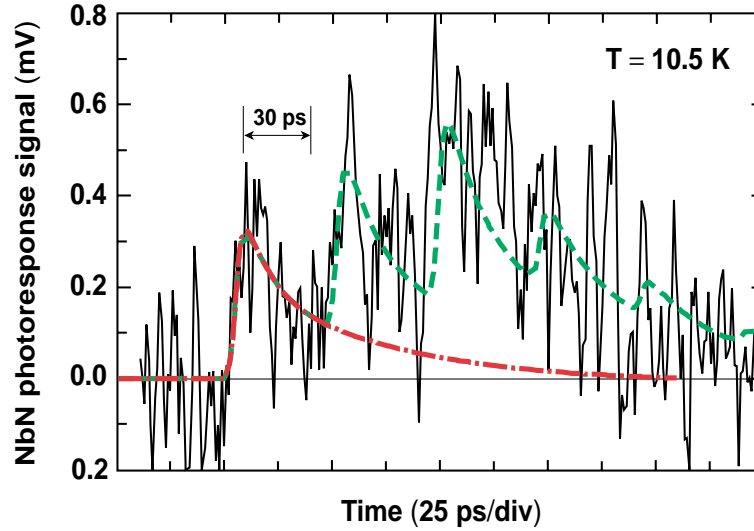


Figure 1. Time resolved response of an NbN HEP to a 100 fs optical excitation pulse. Temperature was 10.5 K.

optical access through a pair of fused-silica windows. To facilitate electro-optic (EO) measurements the entire waveguide structure was overlaid with an EO LiTaO₃ crystal. The EO sampling experimental setup and the method of transient response measurements of superconducting films are described in detail in [5]. The measurement system that we used to study the response sensitivity of samples to near-infrared radiation ($\lambda = 0.79 \mu\text{m}$), including the signal-detection circuitry, laser-diode bias, fibre-optic beam delivery and the NbN HEP, is presented in [6].

3. Results and discussion

3.1. Time response

A typical response of our HEP, consisting of 25 parallel, $2 \mu\text{m}$ wide stripes, measured with the EO sampling technique is presented in figure 1. We note that the signal (thin full curve) contains a large amount of noise, but it was acquired at low bias current, $175 \mu\text{A}$, and at a temperature of 10.5 K, just at the superconducting–resistive transition. The chain curve represents the response of the sample for the single-pulse input, calculated based on the two-temperature (2T) model [7]. Since the reflection-free time window for our experiments, because of the limited length of the CPW and large signal propagation velocity on sapphire, was below 40 ps, the reflections from the CPW ends contributed to the response measured by the EO sampling and had to be included in simulations. The broken curve in figure 1 shows the result of our 2T model calculations that considered those reflections. The fit allowed us to determine the inelastic electron–phonon interaction time $\tau_{e-ph} = 10 \pm 2$ ps and phonon escape time $\tau_{es} \approx 40$ ps. While τ_{e-ph} represents the intrinsic response time of the NbN HEP, the actual device decay time, which is given by the time that elapses from the pulse arrival until the magnitude of the response decreases to $1/e$ from its maximum value (see figure 1), was 30 ps (27 ± 5 ps). In [8], we indicated several possible ways to reduce the effective 30 ps device response time to the intrinsic 10 ps value.

3.2. Efficiency and responsivity

Figure 2 shows the dependence of the ac-measured photoresponse signal on the bias current, $\Delta U(I)$, overlaid with the current–voltage (I – V) curve. The device was irradiated with the ac-modulated CW light from a laser diode and kept at $T = 11.4$ K, which corresponded to the superconducting transition, near the maximum value of the dR/dT curve. The data presented in figure 2 are for the HEP that consisted of five parallel stripes, $6 \mu\text{m}$ long and $0.6 \mu\text{m}$ wide. The dependence $\Delta U(I)$ shows that the maximum value of the photoresponse $\Delta U_{max} = 20 \mu\text{V}$ is for $I = 190 \mu\text{A}$, which corresponds to the resistive nonlinear part of the HEP I – V characteristics with differential resistance $R_{opt} = 168 \Omega$. Simultaneously, we have verified that ΔU_{max} also corresponded to the maximum of the dR/dT curve (approximately $250 \Omega \text{K}^{-1}$ at 11.4 K), calculated from the R versus T dependence, with the $190 \mu\text{A}$ current bias. The power of laser radiation absorbed by the film P_{abs} was estimated from the following relation:

$$P_{abs} = 4P_1(S_d/S_1)(R_s/Z_0)/[(R_s/Z_0)(n+1)+1]^2 \quad (1)$$

where n is the index of refraction, S_d is the area of the HEP, S_1 is the area of the radiation spot and $Z_0 = 377 \Omega$ is the free-space impedance. Using equation (1), we obtain that for $P_1 = 0.3 \text{ mW}$ incident on the sample whose response is presented in figure 2, $P_{abs} \approx 5.3 \times 10^{-10} \text{ W}$. The absorbed power allowed us to calculate at ΔU_{max} both the voltage $R_V = \Delta U_{max}/P_{abs}$ (V W^{-1}) and current $R_I = (\Delta U_{max}/R_{opt})/P_{abs}$ (A W^{-1}) responsivities, which are $R_V \approx 4 \times 10^4 \text{ V W}^{-1}$ and $R_I \approx 220 \text{ A W}^{-1}$, respectively. Please note that the latter value is significantly higher than the best A W^{-1} responsivity obtained by any semiconductor photodetector.

The HEP quantum efficiency can be explained within the simple model of relaxation processes in a thin superconducting film, schematically illustrated in figure 3. For the superconducting strip in the resistive state, we observe a viscous flux flow; thus, we have in the film both the

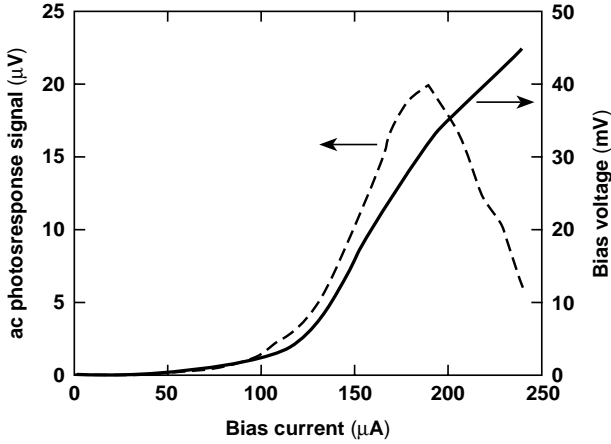


Figure 2. Photoresponse (broken curve) and I - V characteristic (full curve) of an NbN HEP exposed to ac-modulated, $0.79 \mu\text{m}$ wavelength radiation. Temperature was 11.4 K .

normal (vortex cores) and superconducting (the remaining area) regions. Within the latter, the superconductivity is substantially suppressed, as at T close to T_c the energy gap (2Δ) is very small. On absorption of a light quantum by either a normal electron or a Cooper pair, the highly excited electron, with an energy close to the incident photon energy, is created (because of the large physical size of a Cooper pair, only one electron absorbs a photon, while the second one becomes a low-energy quasiparticle). Next, this excited (very hot) electron rapidly (on $<0.1 \text{ ps}$ time scale, according to optical pump-probe experiments [9]) starts to lose its energy via electron–electron scattering and creation of secondary excited electrons. At energies of the order of 0.1 eV (near the Debye temperature), the most efficient mechanism for redistribution of energy within the electron subsystem becomes emission of Debye phonons by electrons. The mean-free path of those phonons is very small, and they efficiently excite additional electrons (break additional Cooper pairs). As the average energy of the electrons in the avalanche decreases to approximately 1 meV ($T \approx 10 \text{ K}$), their further multiplication due to absorption of phonons is replaced by multiplication due to electron–electron collisions, either in the quasiparticle–quasiparticle or quasiparticle–Cooper-pair form. The global T_e is established somewhat above the sample lattice temperature, and the corresponding thermalization time is $\tau_{et} \sim 7 \text{ ps}$ [10]. Further cooling of the electron subsystem toward the lattice temperature occurs via the electron–phonon interaction by emitting thermal phonons, to which the film is transparent.

Since for our NbN films, τ_{es} is significantly longer than τ_{et} and, simultaneously, is shorter than the time of the phonon–electron reabsorption time τ_{ph-e} [8], initially the whole energy of the light quantum $h\nu$ remains in the electron subsystem, redistributing within it and contributing to the elevated T_e . Thus, in this case, the multiplication rate of the electrons may reach the low-temperature value $N_q = h\nu/\Delta(0)$, which for the NbN HEP excited with $0.79 \mu\text{m}$ radiation is $N_q \approx 250$. On the other hand, if we estimate the number of excessive quasiparticles and the effective quantum efficiency of our samples according to the formula used for semiconductor devices, $N_q = (\Delta N_{max}/R_{opt}h\nu/eP_{abs})$, where e is the

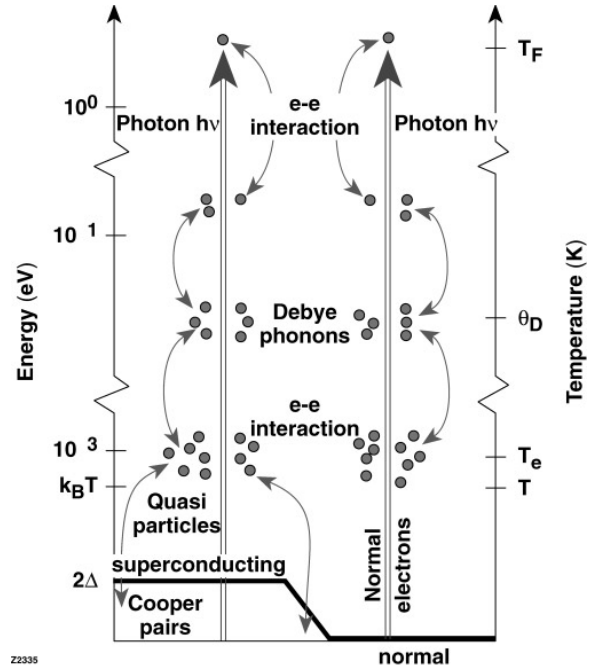


Figure 3. Schematics of the energy thermalization–relaxation process in a superconducting film in the flux-flow state (resistive state, where both the superconducting and normal phases coexist) exposed to optical photons.

electron charge, we obtain a value of ~ 340 for the sample shown in figure 2. The fact that the latter N_q value exceeds the former value is a simple consequence of the fact that at our operating temperature 2Δ is substantially suppressed (much smaller than $2\Delta(0)$).

4. Conclusion

In this work, we have demonstrated that NbN HEPs exhibit device responsivity $R_V \approx 4 \times 10^4 \text{ V W}^{-1}$ or $R_I \approx 220 \text{ A W}^{-1}$, much higher than that for semiconductor photodetectors. Simultaneously, the effective quantum efficiency reaches 340, demonstrating a very large intrinsic gain of the device. The above parameters show that the NbN HEPs should be able to detect single quanta of far-infrared radiation and successfully compete as single-photon detectors with SIS tunnel devices. One can also use HEPs as picosecond optoelectronic input transducers for feeding optically coded information into superconducting integrated digital circuits based on the rapid-single-flux-quantum (RSFQ) logic [11]. Thin-film HEP elements, manufactured as planar, microbridge-type structures, are only several μm in size and can be easily impedance matched with the input of the RSFQ circuit, as well as coupled to standard, single-mode fibres. Finally, the manufacturing methods of the HEP single-layer-film element are well established [4] and are much less involved than those for multilayer SIS elements.

Acknowledgments

This work was supported by the US Office of Naval Research Grant N00014-97-1-0696, the Russian Programme for the

Physics of Condensed Matter (Superconductivity Division) under the grant 94043, and the NATO Linkage Grant CRC.LG974662. The authors thank B M Voronov and E M Menstchekov for their assistance in fabrication of the devices, and C Williams for his help in experiments.

References

- [1] Ejeckam F E, Chua C L, Zhu Z H, Lo Y H, Hong M and Bhat R 1995 *Appl. Phys. Lett.* **67** 3936
- [2] Levine D F 1992 *J. Appl. Phys.* **74** 1993
- [3] Ikegami T 1992 *Proc. IEEE* **80** 411
- [4] Chou S Y, Liu Y, Khalil W, Hsiang T Y and Alexandrou S 1995 *Appl. Phys. Lett.* **61** 819
- [5] Yagoubov P, Gol'tsman G, Voronov B, Seidman L, Siomash V, Cherednichenko S and Gershenson E 1996 *Proc. 7th Int. Symp. on Space Terahertz Technology* p 290
- [6] Lindgren M, Currie M, Williams C, Hsiang T Y, Fauchet P M, Sobolewski R, Moffat S H, Hughes R A and Preston J S 1996 *IEEE J. Sel. Top. Quantum Electron.* **2** 668
- [7] Il'in K S, Milostnaya I I, Verevkin A A, Gol'tsman G N, Gershenson E M and Sobolewski R 1998 *Appl. Phys. Lett.* **73** 3938
- [8] Semenov A D, Nebosis R S, Gousev Y P, Heusinger M A and Renk K F 1995 *Phys. Rev. B* **52** 581
- [9] Il'in K S, Gol'tsman G N, Voronov B M and Sobolewski R 1999 *Proc. 10th Int. Symp. on Space Terahertz Technology (Charlottesville, VA)* p 390
- [10] Gong T, Zheng L X, Xiong W, Kula W, Kostoulas Y, Sobolewski R and Fauchet P M 1993 *Phys. Rev. B* **47** 14 495
- [11] Il'in K S, Lindgren M, Currie M, Sobolewski R, Cherednichenko S I, Semenov A, Gol'tsman G N and Gershenson E M *Appl. Phys. Lett.* submitted
- [12] Likharev K K and Semenov V K 1991 *IEEE Trans. Appl. Supercond.* **1** 3